Supporting information for the manuscript:

Graphene-supported Au-Pd bimetallic nanoparticles with excellent catalytic performance in selective oxidation of methanol to methyl formate

Ruiyi Wang [a,c], Zhiwei Wu [a], Chengmeng Chen [b], Zhangfeng Qin [a,*], Huaqing Zhu [a], Guofu Wang [a], Hao Wang [a], Chengming Wu [a,c], Weiwen Dong [a,c], Weibin Fan [a], Jianguo Wang [a,*]

[a] *State Key Laboratory of Coal Conversion, Institute of Coal Chemistry, Chinese Academy of Sciences, P.O. Box 165, Taiyuan, Shanxi 030001, PR China*

[b] *Key Laboratory of Carbon Materials, Institute of Coal Chemistry, the Chinese Academy of Sciences, P.O. Box 165, Taiyuan 030001, PR China*

[c] *University of Chinese Academy of Sciences, Beijing 100049, PR China*

I. More Experimental Details:

Catalyst preparation: Graphene used here was obtained by rapid heating up of graphene oxide (GO) under high vacuum [1], where GO was synthesized by a modified Hummers' method [2]. The as-prepared GO was grounded into fine powder (300 mesh) and

* Corresponding authors. Tel.: +86-351-4046092; Fax: +86-351-4041153.
E-mail address: qzhf@sxicc.ac.cn (Z. Qin); iccjgw@sxicc.ac.cn (J. Wang)

Postal Address: Prof. Jianguo WANG; Prof. Zhangfeng QIN
State Key Laboratory of Coal Conversion
Institute of Coal Chemistry, Chinese Academy of Sciences
P. O. Box 165
Taiyuan, Shanxi 030001
PR China

loaded into a quartz tube. It was then evacuated to a pressure lower than 2.0 Pa and heated quickly to 200 °C at a rate of 30 °C/min; the graphene sample of fluffy black powder was then generated through the abrupt expansion of GO at about 200 °C.

Au-Pd/Graphene catalysts were prepared by deposition-precipitation method. Briefly, graphene was dispersed in an aqueous solution of sodium carbonate located in water bath of 60 °C; after stirring for 20 min, a mixed aqueous solution of $HAuCl_4 \cdot 3H_2O$ and $PdCl_2$ was added slowly. The mixture was then stirred rigorously for 2.5 h; the resultant Au-Pd/Graphene catalysts were filtered and washed with deionized water until no Cl^- was detected by the solution of $AgNO_3$. After that, the catalysts were dried at 120 °C in vacuum for 3 h and then calcined at 200 °C in air for another 3 h. Other Au-Pd catalysts with different supports (Au-Pd/Al_2O_3, Au-Pd/TiO_2, Au-Pd/CNTs, and Au-Pd/Graphite) or single metal catalyst (Au/Graphene and Pd/Graphene) were also obtained through the similar process.

Catalyst characterizations: The high resolution transmission electron microscopy (HRTEM) images of the catalysts were obtained by a JEM 2010 microscope operating at 200kV. The mean particles size is estimated from a statistic result of 300 particles randomly selected in the images.

The scanning electron microscopy (SEM) image to characterize the surface morphologies of the as-prepared samples were performed on a Field Emission Scanning Electron Microscope (FESEM, JSM 7001-F, JEOL, Japan).

The powder X-ray diffraction (XRD) patterns of the catalysts were collected on a Rigaku MiniFlex II desktop X-ray diffractometer with CuKα radiation source. The measurements were made in the 2θ range from 5° to 80° with a scanning rate of 4 °/min.

The X-ray photoelectron spectroscopy (XPS) spectra were taken on a Thermo ESCALAB 250 instrument with an Al Kα monochromator X-rays source ($h\gamma$ = 1486.6 eV); approximate 100 mg of the powder sample was compressed into a wafer for the measurements.

The BET surface area of the catalysts were measured by nitrogen adsorption at –195.7 °C with a physisorption analyzer (ASAP 2000, Micromeritics Instrument Co., USA). The samples were degassed at 200 °C and 6.7 Pa for 2 h prior to the measurement.

Extended X-ray absorption fine structure spectroscopy (EXAFS) measurements were performed at the beam line BL14W1 of Shanghai Synchrotron Radiation Facility, China. The storage ring energy was 3.5 GeV, and the ring current was 300 mA. The Au L_3 edge data were recorded in a fluorescence mode and the EXAFS data were processed and fitted by using the IFEFFIT package. Fourier transforms to *R* space of the k^3-weighted EXAFS data was performed in the *k* range using the Gaussian window function. Several parameters describing the electronic properties and local structural environment (coordination numbers (*N*), bond lengths (*R*), and their mean squared relative deviations σ^2) around absorbing atoms were determined.

Catalytic Tests: The catalytic performance of Au-Pd/Graphene in methanol oxidation was tested in a quartz fixed-bed microreactor with an inner diameter of 6 mm, as illustrated in Fig. S1. Methanol was introduced into the reactor by bubbling argon via a glass saturator filled with methanol kept at 30 °C. Oxygen was then mixed with the stream carrying methanol vapor. In each test, 0.06 g Au-Pd/Graphene mixed with 1 ml quartz sand was loaded. The products were analyzed on-line by a gas chromatography (GC) equipped with a Porapak-T column and a thermal conductivity detector (TCD). The gas lines were kept at 110 °C to prevent any reactants and products from condensation (Fig. S1)

The products consist of CH_3OH, MF and CO_2. The conversion of methanol x_{MeOH} is determined by

$$x_{MeOH} = (n_{MeOH,feed} - n_{MeOH,outlet})/n_{MeOH,feed} \times 100\% \quad (1)$$

and the selectivity to each product (s_i) is determined by

$$s_i = (n_{i,outlet} \times k_i)/(n_{MeOH,feed} - n_{MeOH,outlet}) \times 100\% \quad (2)$$

where k_i is the carbon number in one molecule of product i.

Turnover frequency (TOF), the number of converted molecules per active site and second, is calculated on the basis of surface Au and Pd atoms, which is estimated with the particle size of Au-Pd nanoparticles and the total loadings of Au plus Pd, i.e.

$$\mathrm{TOF} = \frac{[\text{Product molecules}]}{[\text{Number of active sites}] \times [\text{Time}]} = \frac{0.5 \times F_{MeOH} \times x_{MeOH} \times s_{MF}}{60 \times 22400 \times w_{cat} \times N_{Au\&Pd}} \quad (3)$$

where F_{MeOH} is the volume flow rate of methanol (in unit of ml/min) and w_{cat} means the mass of the catalyst loaded in the reactor (in the unit of g) and $N_{Au\&Pd}$ (g^{-1}) means the number of surface Au and Pd atoms of Au-Pd nanoparticles per gram catalyst.

The SEM and TEM images of the Au-Pd/Graphene catalysts indicate that the gold and palladium nanoparticles dispersed on the support are in a spherical form with a diameter of about 7.5 nm. By assuming the surface metal atoms on the Au and Pd particles as the active sites, and the ratio (γ) of surface atoms for each Au and Pd particle with a radius (r_p) of 3.75 nm is estimated as:

$$\gamma_{Au} = \frac{\frac{4}{3}\pi r_p^3 - \frac{4}{3}\pi\left(r_p - d_{Au}\right)^3}{\frac{4}{3}\pi r_p^3} = \frac{r_p^3 - \left(r_p - d_{Au}\right)^3}{r_p^3} = \frac{3.75^3 - (3.75 - 0.288)^3}{3.75^3} = 0.213 \quad (4)$$

$$\gamma_{Au} = \frac{r_p^3 - (r_p - d_{Pd})^3}{r_p^3} = \frac{3.75^3 - (3.75 - 0.276)^3}{3.75^3} = 0.205 \quad (5)$$

and then

$$N_{Au\&Pd} = \frac{L_{Au} \cdot \gamma_{Au}}{M_{Au}} + \frac{L_{Pd} \cdot \gamma_{Pd}}{M_{Pd}} \quad (6)$$

where L_{Au} and L_{Pd} mean the loadings of Au and Pd (wt.%), respectively; M_{Au} and M_{Pd} means the molar mass of Au and Pd, respectively.

Finally, the TOF value can be estimated by

$$TOF = \frac{0.5 \times F_{MeOH} \times x_{MeOH} \times s_{MF}}{60 \times 22400 \times w_{cat} \times \left(\frac{L_{Au} \cdot \gamma_{Au}}{M_{Au}} + \frac{L_{Pd} \cdot \gamma_{Pd}}{M_{Pd}} \right)} \quad (7)$$

For all catalytic tests, the volume gas flow of methanol was set to 2.75 ml/min. As an example for the methanol oxidation over $Au_{2.0}$-$Pd_{1.0}$/Graphene at 70 °C with 90.2% methanol conversion and 100.0% selectivity to MF, as the loadings of gold and palladium are 2 wt.% and 1 wt.%, respectively, and 60 mg catalyst is used in the test, the TOF can be calculated as:

$$TOF = \frac{0.5 \times 2.75 \times 0.902 \times 1}{60 \times 22400 \times 0.06 \times \left(\frac{0.02 \times 0.213}{197.0} + \frac{0.01 \times 0.205}{106.4} \right)} = 0.377\ s^{-1} \quad (8)$$

II. More Results of Catalyst Characterization and Reaction Tests:

Catalyst preparation: The graphene support used here was obtained by vacuum promoted thermal expansion of graphene oxide (GO) at a relatively low temperature (ca. 200 °C), so as to maintain a high density of oxygen-containing functionalities (e.g. hydroxyl,

epoxy, carboxyl and carbonyl groups) on the surface [3]; the functionalized groups can enhance the hydrophilicity of graphene, which is of benefit to get a uniform dispersion of metal nanoparticles on the surface of the graphene support [4].

Nitrogen adsorption and desorption isotherms for $Au_{2.0}$-$Pd_{1.0}$/Graphene catalyst: The physical adsorption and desorption isotherms of nitrogen on the $Au_{2.0}$-$Pd_{1.0}$/Graphene catalyst are shown in Fig. S2. The $Au_{2.0}$-$Pd_{1.0}$/Graphene has a BET surface area of 194 m^2/g, which is far lower than the theoretical one of completely exfoliated and isolated graphene sheets (ca. 2,620 m^2/g), due to the agglomeration of the graphene oxide sheets upon reduction and loading of Au and Pd [5]. The shape of nitrogen adsorption/desorption isotherms indicate that the $Au_{2.0}$-$Pd_{1.0}$/Graphene catalyst owns both micro- and meso-pores (Fig. S2).

XRD patterns of various catalysts: The XRD patterns of Graphene, $Au_{2.0}$/Graphene, $Au_{2.0}$-$Pd_{1.0}$/Graphene and $Pd_{1.0}$/Graphene are shown in Fig. S3. The graphene support used here displays a typical broaden peak at about 25.0° in its X-ray diffraction (XRD) pattern (Fig. S3), indicating that graphene is present as small crystallites in a single layer or several layers [6]. Comparatively, $Au_{2.0}$/Graphene and $Au_{2.0}$-$Pd_{1.0}$/Graphene show peaks at 38.4°, 44.6°, and 65.1° (Fig. S3), which are assigned to Au(111), Au(200), Au(220), respectively [7]; there are no diffraction peaks detected for palladium species in $Au_{2.0}$-$Pd_{1.0}$/Graphene, possible due to its high dispersion.

XPS spectra of various catalysts: Fig. S4 shows the X-ray photoelectron spectroscopy (XPS) spectra of $Au_{2.0}$/Graphene, $Pd_{1.0}$/Graphene, $Au_{2.0}$-$Pd_{1.0}$/Graphite, $Au_{2.0}$-$Pd_{1.0}$/CNTs and $Au_{2.0}$-$Pd_{1.0}$/Graphene. For $Au_{2.0}$/Graphene in the Au 4*f* region, the fitting curve peaks around the binding energies (BEs) of 84.1 and 87.7 eV are attributed to the Au^0 $4f_{7/2}$ and $4f_{5/2}$, respectively, while the peaks at 85.4 and 89.4 eV are assigned to ionic gold species $Au^{\delta+}$ [8].

Compared with that of $Au_{2.0}$/Graphene, the Au^0 $4f_{7/2}$ peaks of $Au_{2.0}$-$Pd_{1.0}$/Graphite, $Au_{2.0}$-$Pd_{1.0}$/CNTs and $Au_{2.0}$-$Pd_{1.0}$/Graphene shift to lower BEs, i.e. from 84.1 to 83.9, 83.7 and 83.6 eV, respectively. For $Pd_{1.0}$/Graphene in the Pd 3*d* region, the peaks at 342.6 and 337.2 eV are attributed to Pd^{2+} species; Pd^0 species is not identified in the spectra, as no reducing agent is used during the catalyst preparation process. Compared with $Pd_{1.0}$/Graphene, the peaks for Pd^{2+} in $Au_{2.0}$-$Pd_{1.0}$/Graphite, $Au_{2.0}$-$Pd_{1.0}$/CNTs and $Au_{2.0}$-$Pd_{1.0}$/Graphene also moves to lower BEs, i.e. from 342.6 to 342.4, 342.2 and 342.0 eV, respectively.

The much lower BEs of both Au and Pd in $Au_{2.0}$-$Pd_{1.0}$/Graphene should be attributed to the electron exchange between Au and Pd, i.e. a synergism between Au and Pd nanoparticles, through which Au loses *d* and gains *s* or *p* electrons while Pd loses *s* or *p* electrons and gains *d* electrons [9,10]. The span of the BE shifts in the XPS spectra reflects the synergism extent of Au-Pd bimetallic nanoparticles; Xu et al. reported a –0.4 eV shift for Au 4*f* and –0.1 eV shift for Pd 3*d* peak in Au-Pd/SiO_2 [11] and Hsu et al. observed a –0.5 eV shift for Pd 3*d*5/2 peak in Au@Pd core-shell nanoparticle, compared with pure Pd [12]. In current work, a maximum shift of –0.5 eV for Au $4f_{7/2}$ and –0.6 eV for Pd 3*d* peak in $Au_{2.0}$-$Pd_{1.0}$/Graphene is observed, much larger than those in other Au-Pd bimetallic catalysts, which means a especially strong synergism between Au and Pd in the Au-Pd/Graphene catalysts. As well known, graphene is provided with excellent electronic conductivity, which may promote the electron exchange between Au and Pd and then enhance the synergy between Au and Pd bimetallic nanoparticles; such a character of $Au_{2.0}$-$Pd_{1.0}$/Graphene should also be of benefit to its catalytic performance in methanol oxidation.

It is noteworthy that the Pd^0 species is detected in the Pd 3*d* spectra of Au-Pd supported catalysts, though there is no reducing agent added during the catalyst preparation process;

the fractions of Pd^0 species in $Au_{2.0}$-$Pd_{1.0}$/Graphite, $Au_{2.0}$-$Pd_{1.0}$/CNTs and $Au_{2.0}$-$Pd_{1.0}$/Graphene estimated by fitting the XPS spectra are 5.0%, 18.0% and 62.7%, respectively. The reduction of PdO should be related to the presence of Au species and nature of the carbonaceous support. The graphene support is rich in π electrons and the Au species acts as an electronic promoter for Pd [13,14], which may promote the transfer of these electrons to the electron-deficient Pd sites and thereon the reduction of PdO, resulting in abundant Pd^0 species in $Au_{2.0}$-$Pd_{1.0}$/Graphene (Fig. S4).

EXAFS spectra of various catalysts: Fig. S5 shows Au L_3 edge EXAFS spectra of the Au foil, $Au_{2.0}$/Graphene, fresh $Au_{2.0}$-$Pd_{1.0}$/Graphene and spent $Au_{2.0}$ $Pd_{1.0}$/Graphene catalysts, together with the lines fitted for the first-shell. The fitted values of the structure parameters are listed in Table S1. It can be observed that the values of $R_{Au\text{-}Au}$ (2.850 Å) and $N_{Au\text{-}Au}$ (9.0) of $Au_{2.0}$/Graphene are decreased, compared with those of Au foil (2.875 Å and 12). The lattice contraction is common for metal nanoparticles, which may be attributed to the surface tension [15]. However, compared with $Au_{2.0}$/Graphene, the values of $R_{Au\text{-}Au}$ (2.838 Å) and $N_{Au\text{-}Au}$ (6.5) of $Au_{2.0}$-$Pd_{1.0}$/Graphene are further decreased. Besides the surface tension, the decrease of $R_{Au\text{-}Au}$ for $Au_{2.0}$-$Pd_{1.0}$/Graphene may also indicate that part of Pd atoms has entered the Au lattice, as the $R_{Pd\text{-}Pd}$ value for Pd foil (2.748 Å) is much smaller than the $R_{Au\text{-}Au}$ value for Au foil (2.875 Å), that is, the partial alloying of Au-Pd may also contribute to the decrease of $R_{Au\text{-}Au}$ in $Au_{2.0}$-$Pd_{1.0}$/Graphene [16,17]. The decrease of the coordination number (N) may reflect the segregation degree of the Au-Pd nanoparticles. The HRTEM results shown below also suggest that the alloy structure may be formed at the junction of Au-Pd twined particles.

Performances of Au-Pd bimetallic catalysts with different supports: The conversion of methanol and selectivity to MF for methanol oxidation over Au-Pd bimetallic catalysts

with different supports over temperature are illustrated in Fig. S6. $Au_{2.0}$-$Pd_{1.0}$/graphene exhibits much higher activity than other catalysts. Over $Au_{2.0}$-$Pd_{1.0}$/graphene, high selectivity to MF can be achieved with high methanol conversion at relatively lower temperature. Over other catalysts, though the methanol conversion increases with the reaction temperature, the selectivity to MF also decreases considerably with the increase of methanol conversion at higher temperature. These suggest that a synergism effect is present between Au and Pd and graphene as a support is superior to Al_2O_3, TiO_2, graphite and carbon nanotubes (CNTs) to embody this synergism effect. Graphene used here as a support is able to anchor the Au-Pd nanoparticles with a uniform dispersion during the catalytic reaction process.

Performances of the Au_m-Pd_n/Graphene catalysts with different Au and Pd loadings: The conversion of methanol and selectivity to MF for methanol oxidation over the Au_m-Pd_n/Graphene catalysts with different Au/Pd loadings over temperature are illustrated in Fig. S7. Obviously, the catalytic performance of Au-Pd/Graphene is also related to the loadings of Au and Pd; the $Au_{2.0}$-$Pd_{1.0}$/Graphene performs best in methanol oxidation to MF, with a methanol conversion of 90.2% and selectivity of 100% to MF at 70 °C.

$Au_{2.0}$-$Pd_{1.0}$/Graphene gives a turnover frequency (TOF) of 0.377 s^{-1} at 70 °C, much higher than the Au-Ag catalyst with a TOF of 0.11 s^{-1} for methanol oxidation at 80 °C, as reported by Wittstock et al. [18], which suggests that the Au-Pd/Graphene catalyst with much lower fraction of noble metal is yet more effective for methanol oxidation to MF than the pure Au-Ag catalyst. Moreover, a combination of 2.0 wt.% Au and 1.0 wt.% Pd loaded on Graphene is sufficient to attain a maximum synergism between Au and Pd nanoparticles (Entry 12, Fig. 1); a further increase of the Au-Pd loadings may lead to lower methanol conversion (Entry 14, with a very low TOF of 0.026 s^{-1}) and much poorer selectivity to MF (only16.3%, most of methanol is converted to CO_2).

Long term test: A long term test of 48 h was conducted over $Au_{2.0}$-$Pd_{1.0}$/Graphene at 70 °C, as shown in Fig. S8. The $Au_{2.0}$-$Pd_{1.0}$/Graphene exhibits a good stability throughout the test; the conversion of methanol remains around 85.0% and the selectivity is fixed at 100% during the whole period.

Material balance: During the long term test of 48 h, only MF and methanol are observed in the effluents (very rarely, trace amount of CO_2 may be detected). To make a material balance, the amount of methanol fed into the reactor was determined by the weight loss of methanol in the glass vapor saturators and the liquid products and unreacted methanol in the effluents were collected in a trap with a dry ice (solid carbon dioxide) bath. By comparing the mass of methanol consumed with that of the products formed, a well carbon mass balance is obtained; the fraction of unclaimed carbon-containing products is less than 4% (Table S2). Moreover, after the test, the weight of the spent Au-Pd/Graphene catalyst is also almost identical to that of the fresh catalyst loaded before the reaction. All these suggest that the formation of other byproducts like any polymers or heavier products is negligible.

A comparison of the fresh $Au_{2.0}$-$Pd_{1.0}$/Graphene catalyst with the spent one: A comparison of the fresh $Au_{2.0}$-$Pd_{1.0}$/Graphene catalyst with the spent one after 48 h long-term test for methanol oxidation in TEM images and size distribution is shown in Fig. S9. The $Au_{2.0}$-$Pd_{1.0}$/Graphene catalyst exhibits a good stability throughout the test; the conversion of methanol remains around 80% and the selectivity is fixed at 100% during the whole period. A comparison of the TEM image of the spent catalyst with that of the fresh one indicates that the Au-Pd bimetallic nanoparticles is stable during the long term test (Fig. S9); the particle size is only increased slightly from 7.4 to 7.9 nm.

Compared with those of the fresh $Au_{2.0}$-$Pd_{1.0}$/Graphene catalyst, the EXAFS results shown in Fig. S5 and in Table S1 also illustrate that the values of $R_{Au\text{-}Au}$ and $N_{Au\text{-}Au}$ of the

used catalyst are almost unchanged, suggesting that the twined Au-Pd Alloy structure is stable during the methanol oxidation under current conditions.

In conclusion, graphene is successfully decorated with Au-Pd bimetallic nanoparticles of about 7.5 nm through deposition-precipitation. $Au_{2.0}$-$Pd_{1.0}$/Graphene with Au loading of 2.0 wt.% and Pd loading of 1.0 wt.% exhibits high catalytic activity in the selective oxidation of methanol to MF by molecular oxygen, with a methanol conversion of 90.2% and selectivity of 100% to MF at 70 °C. The excellent catalytic performance may be ascribed to the synergism of Au and Pd particles as well as the strong interaction between graphene and Au-Pd nanoparticles.

References

[1] W. Lv, D.M. Tang, Y.B. He, C.H. You, Z.Q. Shi, X.C. Chen, C.M. Chen, P.X. Hou, C. Liu, Q.H. Yang. Low temperature exfoliated graphenes: vacuum-promoted exfoliation and electrochemical energy storage. ACS Nano 2009, 3, 3730–3736.

[2] C.M. Chen, Q.H. Yang, Y. Yang, W. Lv, Y. Wen, P.X. Hou, M. Wang, H.M. Cheng. Sel-assembled free-standing graphite oxide membrane. Adv. Mater. 2009, 21, 3007–3011.

[3] C.M. Chen, Q. Zhang, M.G. Yang, C.H. Huang, Y.G. Yang, M.Z. Wang. Structure evolution during annealing of thermally reduced graphene nanosheets for application in supercapacitors. Carbon 2012, 50, 3572–3584.

[4] C. Xu, X. Wang, J. Zhu. Graphene-Metal Particle Nanocomposites. J. Phys. Chem. C 2008, 112, 19841–19845.

[5] S. Stankovich, D.A. Dikin, R.D. Pinker, K.A. Kohlhaas, A. Kleinhammes. Y.Y. Jia, Y. Wu, S.T. Nguyen, R.S. Ruoff. Synthesis of graphene-based nanosheets via chemical

reduction of exfoliated grahite oxide. Carbon 2007, 45, 1558–1565.

[6] C.F. Chang, Q.D. Truong, J.R. Chen. Graphene sheets synthesized by ionic-liquid assisted electrolysis for application in water purification. Appl. Surf. Sci. 2013, 264, 329–334.

[7] H. Zhu, Z. Ma, J.C. Clark, Z, Pan, S.H. Overbury, S. Dai. Low temperature CO oxidation on Au/fumed SiO_2-based catalyst prepared from $Au(en)_2Cl_3$ precursor. Appl. Catal. A 2007, 326, 89–99.

[8] D.A. Bulushev, I. Yuranov, E.I. Suvorova, P.A. Buffat, L. Kiwi-Minsker. Highly dispersed gold on activated carbon fibers for low temperature CO oxidation. J. Catal. 2004, 224, 8–17.

[9] J. Xu, T. White, P. Li, C.H. He, J.G. Yu, W.K. Yuan, Y.F. Han. Biphasic Pd-Au alloy catalyst for low-temperature CO oxidation. J. Am. Chem. Soc. 2010, 132, 10398–10406.

[10] Y.S. Lee, Y.S. Jeon, Y.D. Chung, K.Y. Lim, C.M. Whang, S.J. Oh. Charge redistribution and electronic behavior in Pd-Au alloys. J. Korea Phys. Soc. 2000, 37, 451–455.

[11] B. Xu, X. Liu, J. Haubrich, R.J. Madix, C.M. Friend. Selectivity control in gold-mediated esterification of methanol. Angew. Chem. Int. Ed. 2009, 48, 4206–4209.

[12] C. Hsu, C. Huang, Y. Hao, F. Liu. Au/Pd core-shell nanopartilces for enhanced electrocatalytic activity and durability. Electrochem. Comm. 2012, 23, 133–136.

[13] M. Sankar, N. Dimitratos, P.J. Miedziak, P.P. Wells, C.J. Kiely, G.J. Hutchings. Designing bimetallic catalysts for a green and sustainable future. Chem. Soc. Rev. 2012, 41, 8099–8139.

[14] P. Kittisakmontree, B. Pongthawornsakun, H. Yoshida, S. Fujita, M. Arai, J. Panpranot. The liquid-phase hydrogenation of 1-heptyne over Pd-Au/TiO2 catalysts prepared by the combination of incipient wetness impregnation and deposition–precipitation. 2013, J. Catal. 2013, 297, 155–164.

[15] A. I. Frenkel, S. Nemzer, I. Pister, L. Soussan, T. Harris, Y. Sun, M. H. Rafailovich. Size-controlled synthesis and characterization of thiol-stabilized gold nanoparticles. J. Chem. Phys. 2005, 123, 184701–184706.

[16] X.W. Teng, Q. Wang, P. Liu, W.Q. Han, A. Frenkel, W. Wen, N. Marinkovic, J.C. Hanson, J.A. Rodriguez. Formation of Pd/Au nanostructures from Pd nanowires via galvanic replacement reaction. J. Am. Chem. Soc. 2008, 130, 1093–1101.

[17] G. Zhang, Y. Wang, X. Wang, Y. Chen, Y. Zhou, Y. Tang, L. Lu, J. Bao, T. Lu, Preparation of Pd–Au/C catalysts with different alloying degree and their electrocatalytic performance for formic acid oxidation. Appl. Catal. B 2011, 102, 614–619.

[18] A. Wittstock, V. Zielasek, J. Biener, C.M. Friend, M. Bäumer. Nanoporous gold catalysts for selective gas-phase oxidative coupling of methanol at low temperature. Science 2010, 327, 319–322.

Captions

Table S1. Results of Au L_3 edge EXAFS fitted the first-shell of the Au foil, $Au_{2.0}$/Graphene, fresh $Au_{2.0}$-$Pd_{1.0}$/Graphene and spent $Au_{2.0}$-$Pd_{1.0}$/Graphene catalysts.

Table S2. Carbon mass balances attained during the long term test of 48 h for methanol oxidation over the $Au_{2.0}$-$Pd_{1.0}$/Graphene catalyst at 70 °C.

Fig. S1. Schematic setup of the apparatus for the catalytic tests of methanol selective oxidation: (1) Purification tube, (2) Mass flow controller, (3) Methanol saturator, (4) Fixed-bed reactor, (5) Six-way wave, and (6) Gas chromatograph.

Fig. S2. Nitrogen adsorption and desorption isotherms of the $Au_{2.0}$-$Pd_{1.0}$/Graphene catalyst.

Fig. S3. XRD patterns of Graphene (a), $Au_{2.0}$/Graphene (b), $Au_{2.0}$-$Pd_{1.0}$/Graphene (c), and $Pd_{1.0}$/Graphene (d).

Fig. S4. Au 4*f* (a) and Pd 3*d* (b) XPS spectra of the $Au_{2.0}$/Graphene (1), $Pd_{1.0}$/Graphene (2), $Pd_{1.0}$/Graphite (3), $Au_{2.0}$-$Pd_{1.0}$/CNTs (4), and $Au_{2.0}$-$Pd_{1.0}$/Graphene (5) catalysts. This Fig. is identical to Fig. 2 in the main manuscript.

Fig. S5. Au L_3 edge EXAFS of the Au foil (a), $Au_{2.0}$/Graphene (b), fresh $Au_{2.0}$-$Pd_{1.0}$/Graphene (c) and spent $Au_{2.0}$-$Pd_{1.0}$/Graphene (d) catalysts. Red dashed lines are those fitted for the first-shell.

Fig. S6. Methanol conversion (I) and selectivity to MF (II) for methanol oxidation over Au-Pd bimetallic catalysts of different supports over the reaction temperature. (a) $Au_{2.0}$-$Pd_{1.0}$/nanotube, (b) $Au_{2.0}$-$Pd_{1.0}$/graphite, and (c) $Au_{2.0}$-$Pd_{1.0}$/graphene. Reaction

conditions: the flow rate of feed stream (6.4 vol.% CH_3OH + 70.2 vol.% O_2 + balanced Ar) is 42.8 ml/min; 60 mg catalyst is used (equivalent to a gas hourly space velocity (GHSV) of 42,800 $ml \cdot g^{-1} \cdot h^{-1}$).

Fig. S7. Methanol conversion (I) and selectivity to MF (II) for methanol oxidation over the Au_m-Pd_n/Graphene catalysts with different Au/Pd loadings. (a) $Au_{1.0}$-$Pd_{0.5}$/Graphene, (b) $Au_{1.0}$-$Pd_{1.0}$/Graphene, (c) $Au_{1.0}$-$Pd_{2.0}$/Graphene, (d) $Au_{2.0}$-$Pd_{1.0}$/Graphene; and (e) $Au_{4.0}$-$Pd_{2.0}$/Graphene. Reaction conditions are the same as those listed in Fig. S4.

Fig. S8. Long-term test of the selective oxidation of methanol over $Au_{2.0}$-$Pd_{1.0}$/Graphene at 70 °C: (a) methanol conversion; (b) selectivity to MF. Reaction conditions: 60 mg catalyst; feed of 6.4 vol.% CH_3OH + 70.2 vol.% O_2 + balanced Ar with a flow rate of 42.5 ml/min.

Fig. S9. Representative TEM images and size distribution of $Au_{2.0}$-$Pd_{1.0}$/Graphene. (a) Fresh catalyst; (b) Spent catalyst; (c) Size distribution of Au and Pd nanoparticles (the solid bars for the fresh catalyst, while the open bars for the spent catalyst after 48 h long-term test for methanol oxidation); d) HR-TEM of the fresh catalyst; e) HR-TEM of the spent catalyst.

Table S1.

Results of Au L_3 edge EXAFS fitted the first-shell of the Au foil, $Au_{2.0}$/Graphene, fresh $Au_{2.0}$-$Pd_{1.0}$/Graphene and spent $Au_{2.0}$-$Pd_{1.0}$/Graphene catalysts.

Samples	$N_{Au\text{-}Au}$	$R_{Au\text{-}Au}$ (Å)	$\sigma^2_{Au\text{-}Au}$ (Å^2)
Au foil	12.0	2.875	-
$Au_{2.0}$/Graphene	9.0	2.850	0.009
$Au_{2.0}$-$Pd_{1.0}$/Graphene, fresh	6.5	2.838	0.020
$Au_{2.0}$-$Pd_{1.0}$/Graphene, spent	6.0	2.832	0.016

Table S2.

Carbon mass balances attained during the long term test of 48 h for methanol oxidation over the $Au_{2.0}$-$Pd_{1.0}$/Graphene catalyst at 70 °C.

Items	Quantity
Feed	
Methanol evaporated in the saturators ($n_{MeOH,in}$, mol)	0.334
Effluents	
MF collected ($n_{MF,out}$, mol)	0.137
Unreacted methanol collected ($n_{MeOH,out}$, mol)	0.050
Water collected ($n_{H2O,out}$, mol)	0.285
Estimated CO_2 formation ($n_{CO2,out}$, mol)	0.0
Unclaimed fraction of carbon-containing products, i.e. $f_C=[(n_{MeOH,in}-n_{MeOH,out})-(2n_{MF,out}+n_{CO2,out})]/(n_{MeOH,in}-n_{MeOH,out})\times100\%$	3.5

Fig. S1.

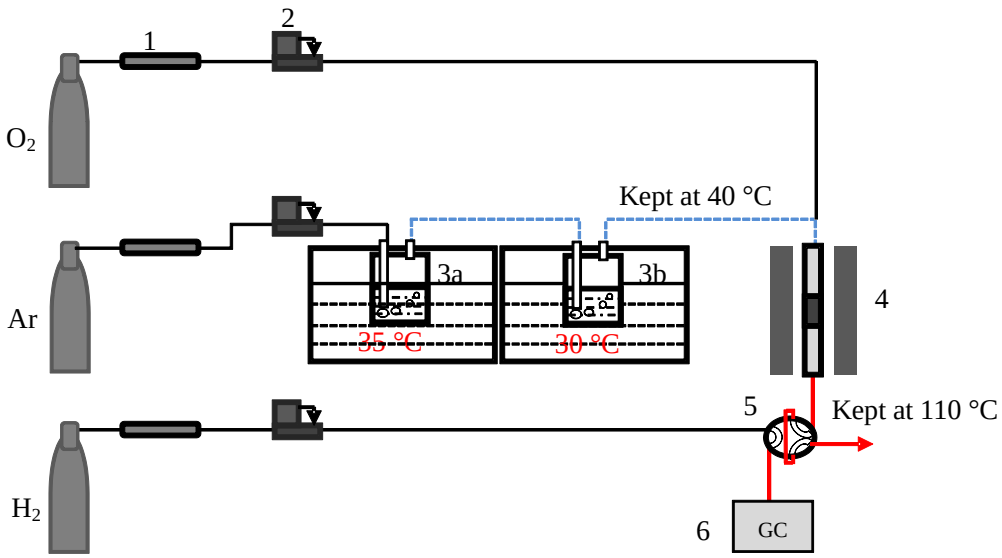

Fig. S1. Schematic setup of the apparatus for the catalytic tests of methanol selective oxidation: (1) Purification tube, (2) Mass flow controller, (3) Methanol saturator, (4) Fixed-bed reactor, (5) Six-way wave, and (6) Gas chromatograph.

Fig. S2.

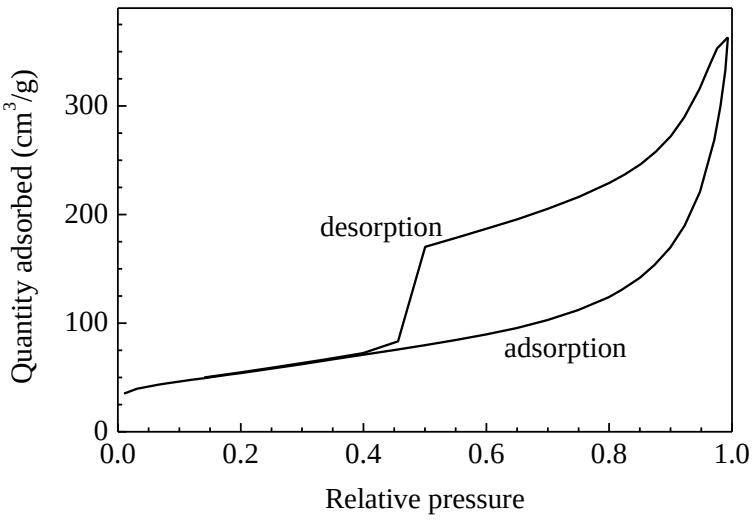

Fig. S2. Nitrogen adsorption and desorption isotherms of the $Au_{2.0}$-$Pd_{1.0}$/Graphene catalyst.

Fig. S3.

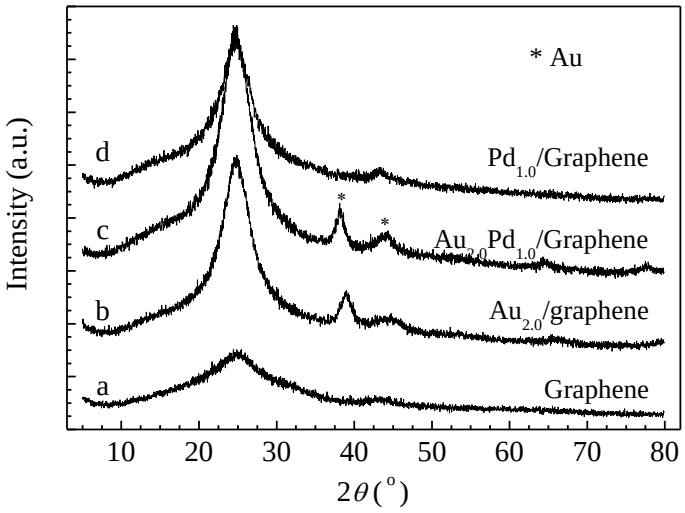

Fig. S3. XRD patterns of Graphene (a), $Au_{2.0}$/Graphene (b), $Au_{2.0}$-$Pd_{1.0}$/Graphene (c), and $Pd_{1.0}$/Graphene (d).

Fig. S4.

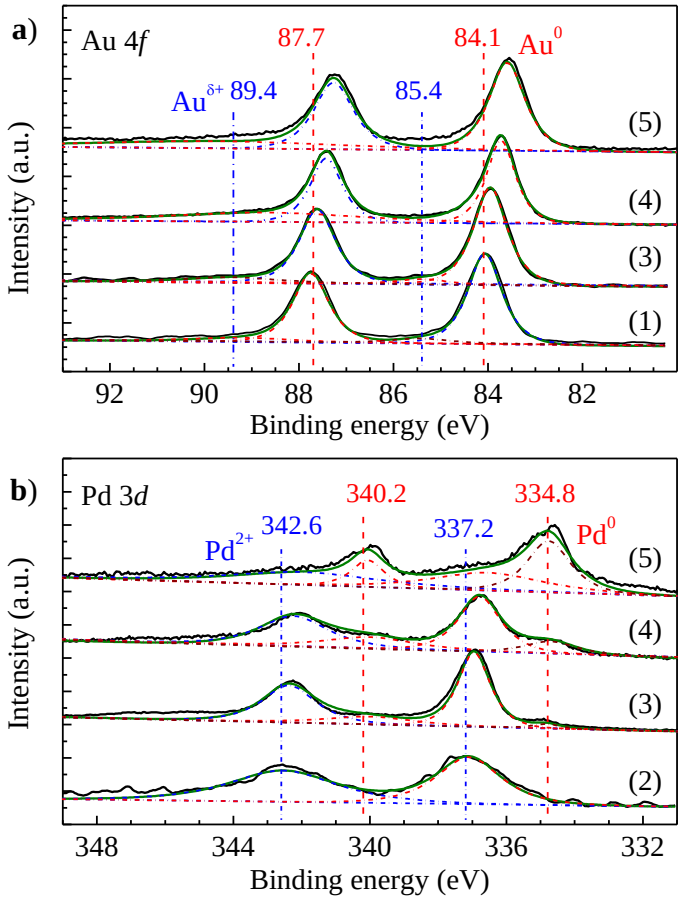

Fig. S4. Au 4*f* (a) and Pd 3*d* (b) XPS spectra of the $Au_{2.0}$/Graphene (1), $Pd_{1.0}$/Graphene (2), $Pd_{1.0}$/Graphite (3), $Au_{2.0}$-$Pd_{1.0}$/CNTs (4), and $Au_{2.0}$-$Pd_{1.0}$/Graphene (5) catalysts. This Fig. is identical to Fig. 2 in the main manuscript.

Fig. S5.

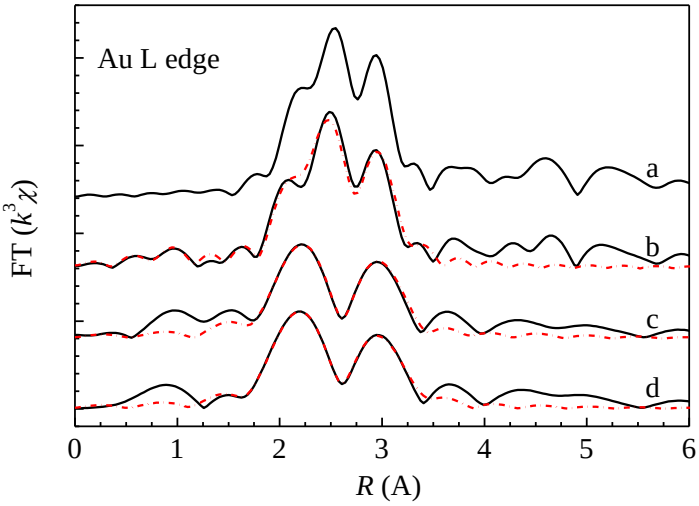

Fig. S5. Au L_3 edge EXAFS of the Au foil (a), $Au_{2.0}$/Graphene (b), fresh $Au_{2.0}$-$Pd_{1.0}$/Graphene (c) and spent $Au_{2.0}$-$Pd_{1.0}$/Graphene (d) catalysts. Red dashed lines are those fitted for the first-shell.

Fig. S6.

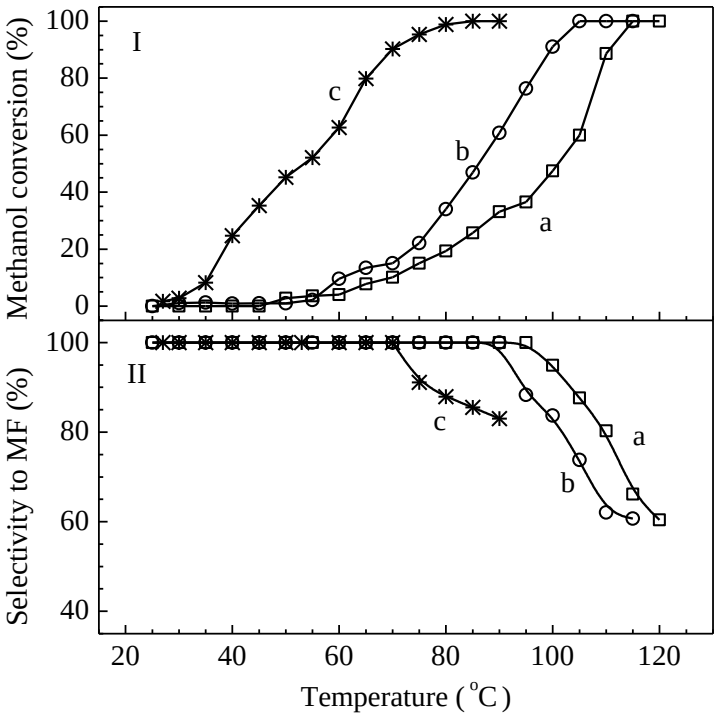

Fig. S6. Methanol conversion (I) and selectivity to MF (II) for methanol oxidation over Au-Pd bimetallic catalysts of different supports over the reaction temperature. (a) $Au_{2.0}$-$Pd_{1.0}$/nanotube, (b) $Au_{2.0}$-$Pd_{1.0}$/graphite, and (c) $Au_{2.0}$-$Pd_{1.0}$/graphene. Reaction conditions: the flow rate of feed stream (6.4 vol.% CH_3OH + 70.2 vol.% O_2 + balanced Ar) is 42.8 ml/min; 60 mg catalyst is used (equivalent to a gas hourly space velocity (GHSV) of 42,800 $ml \cdot g^{-1} \cdot h^{-1}$).

Fig. S7.

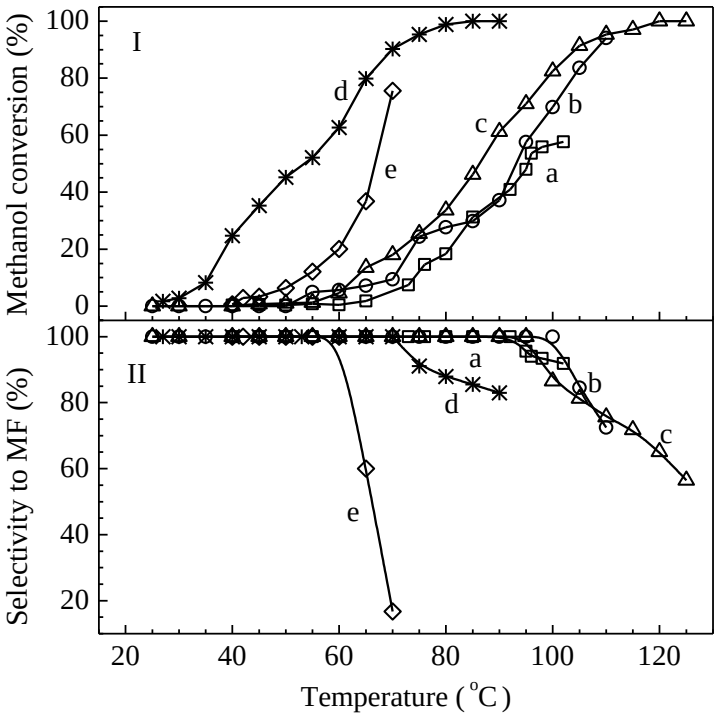

Fig. S7. Methanol conversion (I) and selectivity to MF (II) for methanol oxidation over the Au_m-Pd_n/Graphene catalysts with different Au/Pd loadings. (a) $Au_{1.0}$-$Pd_{0.5}$/Graphene, (b) $Au_{1.0}$-$Pd_{1.0}$/Graphene, (c) $Au_{1.0}$-$Pd_{2.0}$/Graphene, (d) $Au_{2.0}$-$Pd_{1.0}$/Graphene; and (e) $Au_{4.0}$-$Pd_{2.0}$/Graphene. Reaction conditions are the same as those listed in Fig. S4.

Fig. S8.

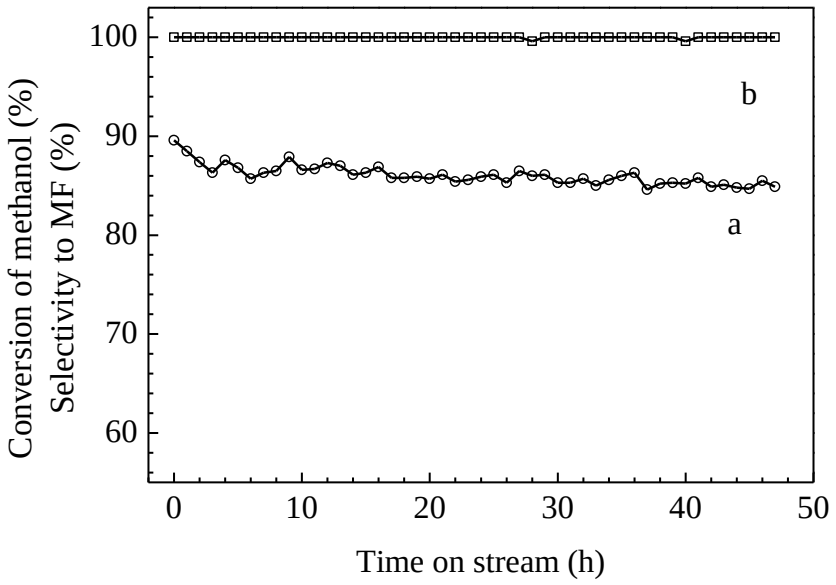

Fig. S8. Long-term test of the selective oxidation of methanol over $Au_{2.0}$-$Pd_{1.0}$/Graphene at 70 °C: (a) methanol conversion; (b) selectivity to MF. Reaction conditions: 60 mg catalyst; feed of 6.4 vol.% CH_3OH + 70.2 vol.% O_2 + balanced Ar with a flow rate of 42.5 ml/min.

Fig. S9.

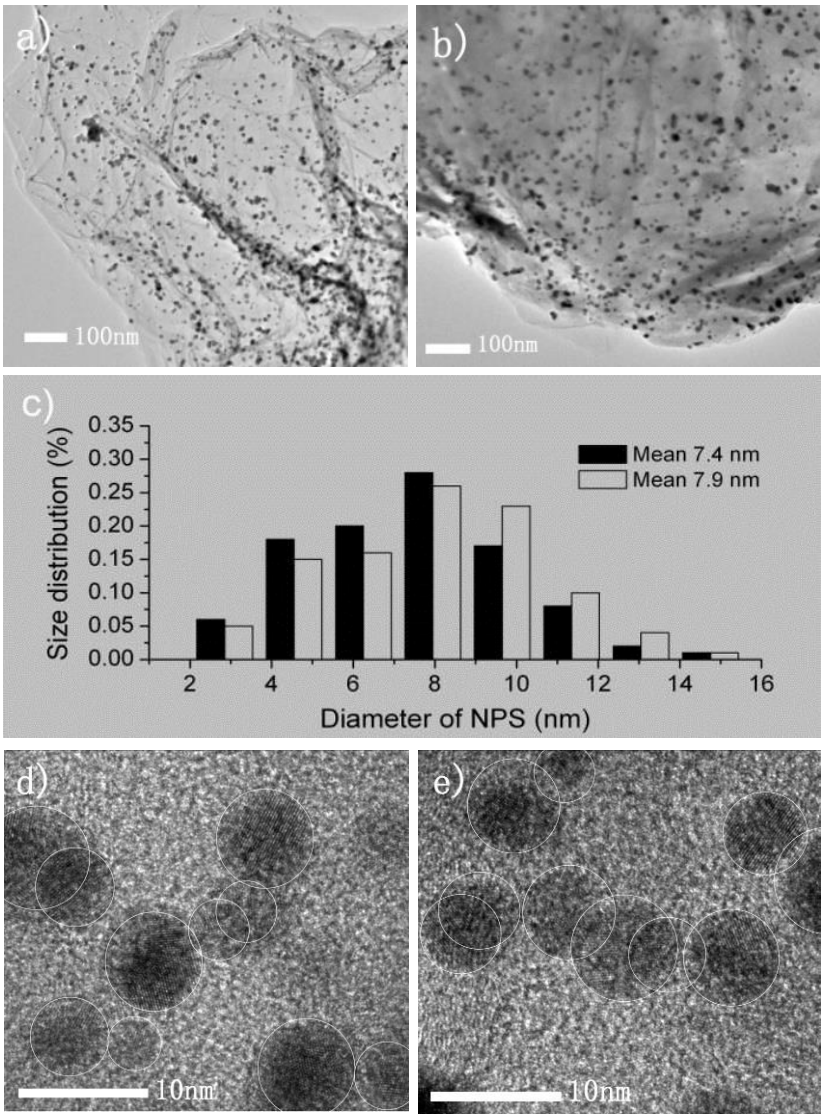

Fig. S9. Representative TEM images and size distribution of $Au_{2.0}$-$Pd_{1.0}$/Graphene. (a) Fresh catalyst; (b) Spent catalyst; (c) Size distribution of Au and Pd nanoparticles (the solid bars for the fresh catalyst, while the open bars for the spent catalyst after 48 h long-term test for methanol oxidation); d) HR-TEM of the fresh catalyst; e) HR-TEM of the spent catalyst.